One-step *in situ* solid-substrate-based whole blood immunoassay based on FRET between upconversion and gold nanoparticles

Cuixia Li[a,b], Jing Zuo[a,b,d], Qiqing Li[a,b], Yulei Chang[a], Youlin Zhang[a,*], Langping Tu[a], Xiaomin Liu[a], Bin Xue[a], Huiying Zhao[c], Hong Zhang[d,*], Xianggui Kong[a,*]

[a] State Key Laboratory of Luminescence and Applications, Changchun Institute of Optics, Fine Mechanics and Physics, Chinese Academy of Sciences, Changchun 130033, China
[b] Graduate University of the Chinese Academy of Sciences, Beijing 100049, China
[c] Department of Basic Medicine, Gerontology Department of First Bethune Hospital, University of Jilin, Changchun 130021, China
[d] Van't Hoff Institute for Molecular Sciences, University of Amsterdam, Science Park 904, 1098 XH Amsterdam, The Netherlands

A R T I C L E   I N F O

A B S T R A C T

Despite their general clinical applications, current fluorescence-based immunoassays are confronted with serious challenges, e.g. the advance serum/ plasma separation and the tedious washing process in current heterogeneous approaches, and aggregation of particles, low sensitivity and the narrow linear range in homogeneous approaches. In this paper, these urgent problems were solved in a novel one-step *in situ* immunoassay of whole blood samples by combining the traditional fluorescence resonance energy transfer (FRET) technology (between upconversion nanoparticles (UCNPs) and gold nanoparticles (GNPs)) and the solid-substrate based immunoassay technology. The low detection limits of goat IgG (gIgG) as 0.042 μg/mL in buffers, 0.51 μg/mL in 20-fold diluted whole blood samples and a wide linear range from 0.75 μg/mL to 60 μg/mL in blood samples were achieved. To the best of our knowledge, it is the first one-step *in situ* solid-substrate-based immunoassay of whole blood samples with large linear detection range. This development provides a promising platform for a rapid and sensitive immunoassay of various bio-molecules directly in whole blood without tedious separation, washing steps and aggregation problems.

1. Introduction

Fluorescence-based immunoassay methods, mainly divided into heterogeneous and homogeneous assays, have been generally applied in current clinics. However, these techniques are constantly suffering from the following problems, *e.g.* aggregation, low sensitivity and narrow linear range in homogeneous assays, as well as the tedious process in heterogeneous assays, which have been not solved (Algar and Krull, 2009; Kim et al., 2009; Kreisig et al., 2011; Ma et al., 2010; Wang et al., 2015; Zhang, 2015). The heterogeneous immunoassay on a solid-support (paper disc, cellulose, microtiter plates, glass or plastic beads, *etc.*), such as enzyme-linked immunosorbent assay (ELISA), is one of the earliest and most mature methods (Apilux et al., 2013; Clark and Adams, 1977; Engvall and Perlmann, 1971). Although, this method is highly sensitive and matches well with the relevant shelf instruments, the serum/ plasma separation of whole blood and the tedious washing processes have to be conducted to avoid strongly fluorescent background and the nonspecific absorption, which not only are labor-intensive and time-consuming, but also may result in the

change of the structure or conformation of the biomolecules and fade of the specificity and sensitivity of the immunoassay (Algar and Krull, 2009; Apilux et al., 2013; Kim et al., 2009; Ma et al., 2010; Noor and Krull, 2013). Confronted by these problems, homogeneous immunoassay methods have been proposed and developed. Most of them were based on FRET principle which is extremely sensitive to the nanoscale changes of distance between energy donors (D) and acceptors (A) and the spectral overlap of the D emission and A absorption (Sapsford et al., 2006; Yun et al., 2005). However, with the solving of the complicated washing/separation problems, new problems emerge such as low sensitivity, narrow linear range and random aggregation of particles (easy to cause some false immunoassay results) (Börner et al., 2011; Chen et al., 2013; Kreisig et al., 2011; Rantanen et al., 2008; Sapsford et al., 2006; Wang et al., 2005, 2015). Therefore, it is imperative to develop novel immunoassay methods which take the advantages of heterogeneous and homogeneous assays, but avoid the serum/ plasma separation, complicated multi-steps process, aggregation of particles. Also important is that it should be compatible with current detection instruments.

---

* Corresponding authors.
  E-mail addresses: zhangyl0109@sina.com (Y. Zhang), h.zhang@uva.nl (H. Zhang), xgkong14@ciomp.ac.cn (X. Kong).

The potential of FRET in solid-substrate-based assays, is dimmed by, for example, the concern that the properties of the energy donor/acceptor are susceptible to environment, which might be the reason behind the fact that only few relevant reports have appeared up to now (Algar and Krull, 2009; Kim et al., 2009) where dyes or GNPs were used as acceptors and quantum dots (QDs) as donors whose properties were easily affected by the interaction of particles and the interaction between particles and the solid surface. Furthermore, the separation problem of serum and the multi-steps washing still remained.

Rare earth ions (RE)-doped UCNPs show excellent fluorescence stability benefiting from the shielding effect of the $5s^2 5p^6$ electronic shell (Tu et al., 2015), which makes them the best candidates of energy donors for solid-substrate-based detection. Moreover, the UCNPs own many other advantages, such as NIR-excitation, narrow emission band, large anti-Stokes shifts (> 300 nm) and no bio-fluorescence. Recently, these nanomaterials have been extensively applied in bio-detection and bio-imaging of complex biological systems, such as plasma, cells, tissues, *etc* (Cen et al., 2015; Chen et al., 2013; Long et al., 2015; Peng et al., 2011, 2015; Wang et al., 2005; Xu et al., 2014). For UCNPs-FRET based detections, GNPs were popularly used as acceptors for a large extinction coefficient and a long FRET half quenching distance (up to 28 nm) (Chen et al., 2013; Long et al., 2015; Peng et al., 2011; Samanta et al., 2014; Wang et al., 2005). However, up to now, UCNPs-FRET based detection was, without exception, executed in solution-based homogeneous immunoassays, which still faced the above-mentioned problems.

Our strategy in this work was to circumvent the above drawbacks of the current immunoassays by innovatively applying UCNPs-based FRET technology (UCNPs as donors, GNPs as acceptors) on a solid-substrate, the novel one-step *in situ* approach on glass substrate realized a direct immunoassay of whole blood samples (gIgG as a proof-of-concept) without any separation and washing steps in the detection. This approach offers a rapid, sensitive, economic and simple operation detection of a variety of bio-molecules directly from whole blood.

2. Materials and methods

2.1. Fabrication of the surface of solid-substrates

To fabricate the bio-functional substrate, the substrates (5 mm×5 mm) were cleaned and functionalized following the procedure of our previous report (Zhang et al., 2010). Briefly, the substrates were firstly cleaned to get rid of the contaminant and activated the hydroxyl. Then, the substrates were immersed in a 10% (v/v) solution of aminopropyltriethoxysilane (APTES) in ethanol for 12 h to form an amino surface. After being rinsed thoroughly and dried in 120 °C oven full of nitrogen, the amino-substrates were modified with 5% glutaraldehyde (GA) solution in methanol containing 0.1 wt% Sodium cyanoborohydride for 12 h to obtain the aldehyde-functionalized substrates. After aldehyde-functionalization, the substrates were immersed in 1 mg/mL polyethyleneimine (PEI)-UCNPs solution containing 0.1 wt% Sodium cyanoborohydride to covalently immobilize UCNPs on the substrates by forming an amine linkage between the aldehyde groups and the amino groups. To obtain a proper surface coverage, the reaction time was set to be 8 h, 12 h, 24 h and 36 h, respectively. To evaluate the immobilized stability of the UCNPs on the substrates, the upconversion fluorescence spectra were measured when the UCNPs-substrates were continuously oscillated in 10 mM PBS buffer for 0 h, 6 h, 12 h, 24 h, 48 h and 96 h, respectively. The UCNPs-substrates were aldehyded again using GA. They were then coated overnight with 0.2 mg/mL rabbit-anti-goat (rIgG) at 4 °C and dipped into 2% bovine serum albumin (BSA) solution for 2 h. Finally, the substrates were immersed in an excess amount of gIgG-GNPs solution with different times from 0 min to 75 min, the upconversion fluorescence spectra were detected. Up to now, the FRET-based bio-functional substrates

have been completely constructed. To verify the stability of the bio-functional substrates, the upconversion fluorescence spectra of the substrates were detected after being kept in 4 °C for 4 h, 12 h, 24 h, 36 h, 48 h and 72 h, respectively.

2.2. Immunoassay in buffers

In the typical FRET-based immunoassay, the constructed bio-functional substrates were vertically inserted into the cuvette containing 10 mM PBS buffers (pH=7.4), and the upconversion fluorescence spectra were recorded. Series concentrations of gIgG (0.09, 0.75, 3.75, 7.5, 15, 30, 45, 60, 75, 90 µg/mL) were prepared, respectively. After reaction, the fluorescence measurements were directly conducted without any washing steps. The schematic diagram of the instrumental setup is shown in Fig. S2. The gIgG concentration can be quantitatively determined according to the recovery of upconversion fluorescence. To obtain the optimum detection time, the fluorescence spectrum was measured every 10 min until the fluorescence was almost unchanged with time. To ensure the precision of the detection, the standard deviations were calculated from four measurements conducted with four independent bio-functional substrates for four samples.

2.3. Specificity of the immunoassay

To determine the detecting specificity, other biomarkers, such as rabbit-anti-human IgG, rabbit IgG, human IgG and BSA, were detected under the same experimental conditions. The concentrations of gIgG, non-specific IgGs and BSA were set as 60 µg/mL, 1 mg/mL and 50 mg/mL, respectively. Meanwhile, for studying the mechanism of the novel immunoassay, the absorption spectra of BSA-gIgG-GNPs (BgGNPs) solutions, BgGNPs bound on rIgG-UCNPs-substrate, BgGNPs bound with rIgG-UCNPs in solution were measured, respectively.

2.4. Immunoassay in whole blood

To evaluate the ability of UCNPs-GNPs-FRET-based approach for whole blood sample assay, the whole blood were firstly thawed at room temperature and mixed well. The immunoassay was performed in 20-fold diluted whole blood. The diluted blood was spiked with a series of concentrations of gIgG (0, 0.75, 1.5, 3.75, 7.5, 15, 30, 45, 60 µg/mL), respectively, and a detection procedure identical to that in buffers was followed.

3. Results and discussion

3.1. Principle of one-step in situ *immunoassay on glass substrate*

UCNPs-GNPs as FRET D-A pair on glass substrates was designed to realize the *in situ* immunoassay and to take advantage of the enrichment effect of the substrate to circumvent the problems of low fluorescent probes concentration and aggregation of nanoparticles in FRET-based homogeneous immunoassay methods. On top of that, the red shift of GNPs absorption spectrum due to the dense assembly on the substrate should encourage better spectral overlap with the emission of UCNPs. The implementation plan of the immunoassay is schematically illustrated in Fig. 1. The UCNPs covalently attached on the substrate are modified by rIgG, and GNPs by gIgG. The specific binding between gIgG and rIgG pushes the donor (UCNPs) and the acceptor (GNPs) in close proximity, which shall result in the fluorescence quenching of UCNPs following mainly FRET mechanism. When the bio-functional substrate is immersed into the analyte (gIgG) solutions, a competitive immunoassay takes place between gIgG-GNPs and free gIgG. Thus, the FRET process is inhibited to some extent, and the fluorescence intensity of UCNPs will be recovered in a gIgG concentration-dependent manner, which is the foundation of the quantitative detection of gIgG.
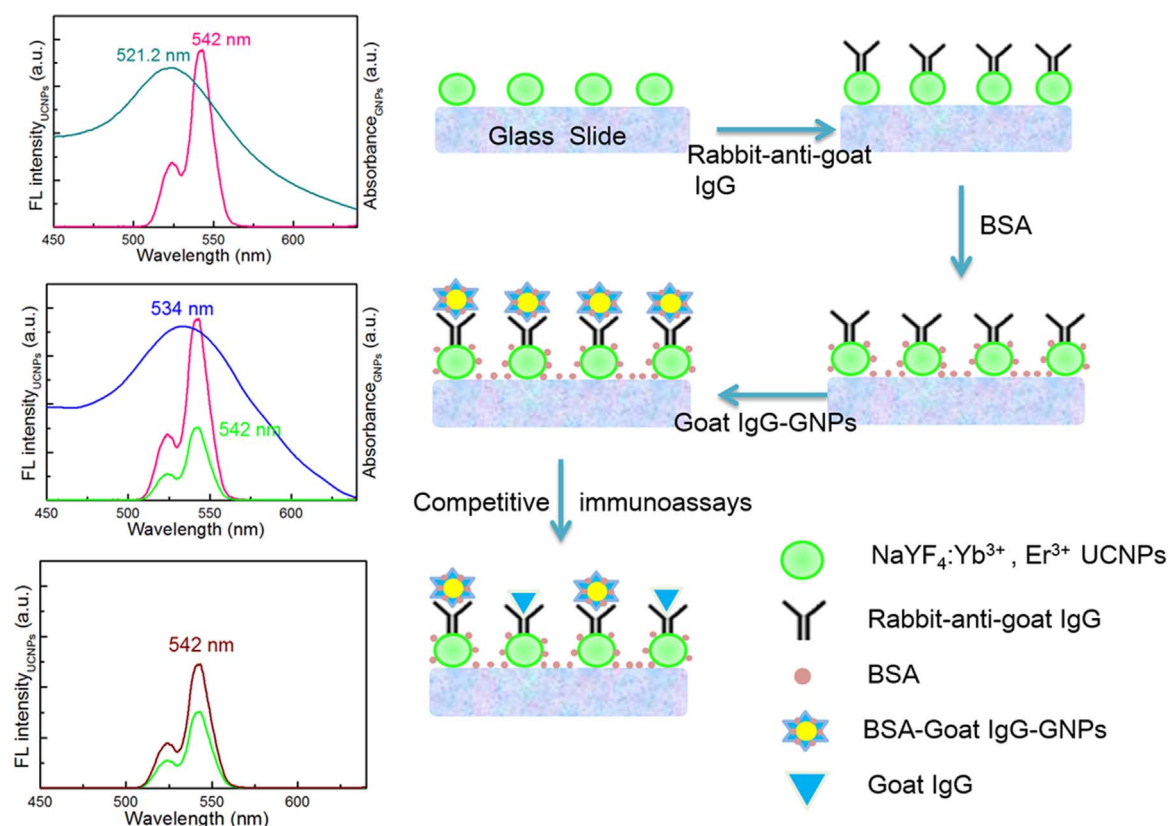
Fig. 1. Schematic illustration of the one-step *in situ* immunoassay based on FRET between UCNPs covalently immobilized on the substrate surface and GNPs for gIgG detection. In the left spectra, the dark green and blue lines represent the absorption spectra of GNPs in water solution and GNPs-IgG-BSA on the substrate, respectively. The pink, light green and red lines represent the emission spectra of the substrate modified with UCNPs (UCNPs-substrate), the UCNPs-substrate further combined with GNPs (before immunoassay) and the substrate after competitive immunoassay, respectively.

3.2. Characterization of NaYF₄:Yb³⁺,Er³⁺ UCNPs and GNPs

For developing the one-step *in situ* FRET-based immunoassay on solid substrate, NaYF₄:Yb³⁺, Er³⁺ UCNPs and GNPs were chosen as the FRET donors and acceptors, respectively. Considering the UCNPs fluorescence efficiency and the influence of the size of UCNPs on FRET efficiency (Krämer et al., 2004; Li et al., 2014), hexagonal UCNPs were prepared, as shown in Fig. 2a-b. The UCNPs are of approximately spherical morphology, mono-dispersed, and uniform with an average size of 22.3 ± 0.8 nm. The diffraction peaks of the UCNPs can be indexed as a pure hexagonal phase of NaYF₄. The oleic acid coated UCNPs were modified with amino-ligand by using PEI as surface coating agent. The surface modification of the UCNPs is verified from FT-IR spectra in Fig. 2c. For OA-UCNPs, the strong peaks of carboxylate anions and methylene group are located at 1466 cm⁻¹, 1557 cm⁻¹ and 2927 cm⁻¹, 2855 cm⁻¹, respectively. After the treatment of hydrochloric solution, the strong peaks at 1466 cm⁻¹, 1557 cm⁻¹, 2927 cm⁻¹ and 2855 cm⁻¹ disappear, indicating that the OA ligands are successfully removed from the surface of OA-UCNPs. After PEI modification, the FT-IR spectrum exhibits a strong characteristic absorption peak of free −NH₂ (1540 cm⁻¹) and the C−N bond (1396 cm⁻¹), as well as a weak peak of amine N−H bending (1641 cm⁻¹), demonstrating that the surface of UCNPs are capped by PEI molecules. Fig. 2f shows the fluorescence spectrum of UCNPs under the excitation of 980 nm. It can be seen that there are three characteristic peaks at 524 nm, 542 nm and 655 nm, originating from the transitions from ²H₁₁/₂, ⁴S₃/₂, and ⁴F₉/₂ excited states to the ⁴I₁₅/₂ ground state, respectively (Zhang et al., 2015).

It is well known that GNPs have a high extinction coefficient and a long FRET half quenching distance (up to 28 nm) (Samanta et al., 2014), which is favorable to assay performances based on FRET. The morphologies of GNPs were analyzed by TEM, as shown in Fig. 2d. GNPs are approximately spherical in shape and relatively uniform in size with a diameter of 15.4 ± 2.2 nm. GNPs show a strong surface plasmon resonance absorption band at 521.2 nm (Fig. 2f). Here, the 542 nm UCNPs emission is chosen as the response spectrum since it shows a better spectral overlap with the absorption of GNPs than 655 nm emission and stronger emission intensity than 524 nm emission. Additionally, it is reported that the GNPs are easy to be conjugated with bio-molecules (Dulkeith et al., 2005; Kreyling et al., 2015; Maxwell et al., 2002). Here, the bio-functional GNPs were constructed by modifying GNPs with gIgG and then blocked with BSA. The successful modification of GNPs was confirmed from the absorption spectra, as shown in Fig. 2e. Red-shifts of absorption spectra from 521.2 nm (GNPs) to 525.7 nm (gIgG-GNPs) and further 527 nm (BSA-gIgG-GNPs) are observed. The red-shifts are attributed to the change of the dielectric constant of the surrounding media. And no obvious peak broadening means well-dispersion and no evident aggregation of GNPs in both cases. Importantly, the red-shifts of absorption spectra caused by modifying GNPs using gIgG and BSA is in favor of a better FRET spectral matching between UCNPs and GNPs to enhance the immunoassay sensitivity of the immunoassay.

3.3. Characterization of the bio-functional solid-substrate

To construct the bio-functional substrate, PEI-UCNPs were covalently modified on APTES-substrates using glutaraldehyde. The immobilization of UCNPs on the substrate with different times (8 h, 12 h, 24 h and 36 h, respectively) were characterized by SEM, as shown in Fig. S3. It is obvious that the longer the reaction time is, the more UCNPs are anchored on the substrate. After reacting for 24 h, the amount of UCNPs immobilized on the substrate reaches saturation.
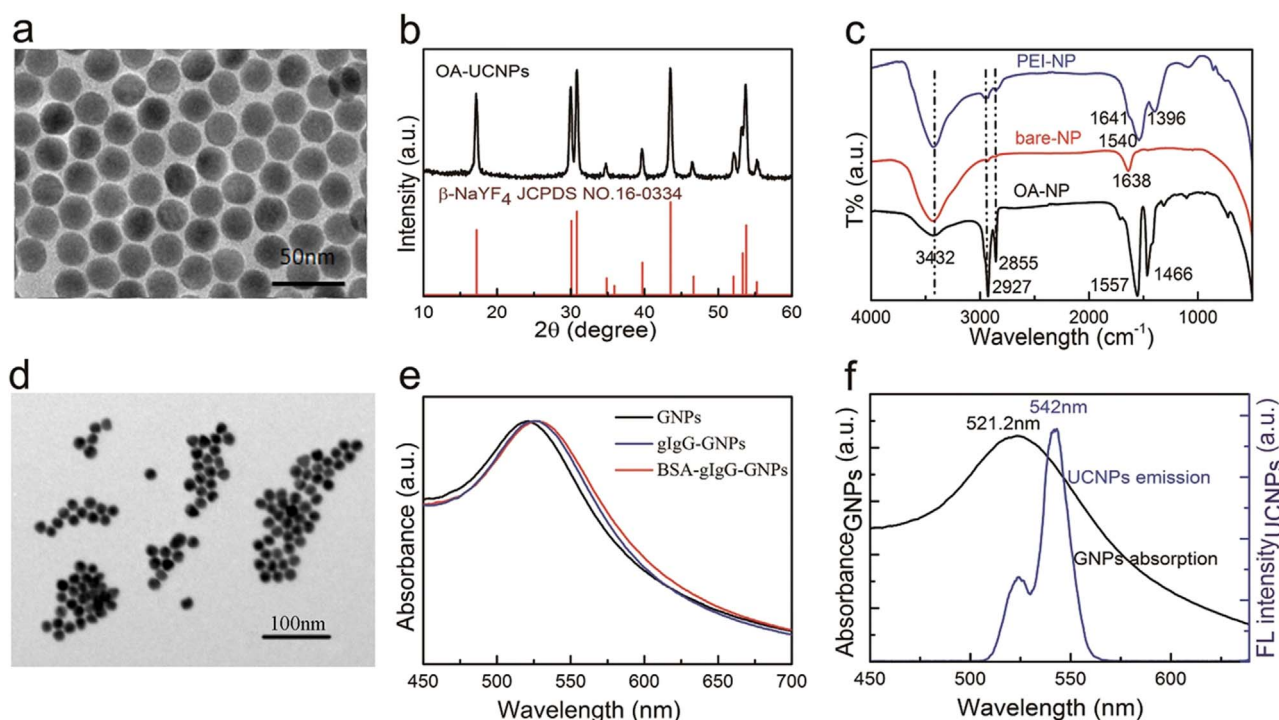
Fig. 2. (**a**) TEM image and (**b**) XRD pattern of NaYF$_4$:Yb^{3+},Er^{3+} UCNPs (black line) and the standard pattern of β-NaYF$_4$ (red line). (**c**) FT-IR spectra of UCNPs: OA-UCNPs (black line), bare-UCNPs (red line) and PEI-UCNPs (blue line). (**d**) TEM image of GNPs. (**e**) Normalized absorption spectra of GNPs (black line), gIgG-GNPs (blue line) and BSA-gIgG-GNPs (red line). (**f**) Fluorescence emission spectrum of UCNPs (blue line) under 980 nm excitation and the SPR absorption spectrum (black line) of GNPs.

AFM imaging was adopted to characterize the immobilization of UCNPs on the glass substrate. The roughness of the bare substrate is about 0.54 nm which is rather smooth, as shown in Fig. S4. The image of UCNPs is shown in Fig. 3a. The height of UCNPs is approximately 21−23 nm, which is consistent with the TEM results, a few nanometers error may result from the tip compression during the imaging process and the substrate itself (Rivetti and Guthold, 1996; Wang et al., 2008; Zeng et al., 2009). The immobilization of UCNPs on the substrate exhibits an excellent monolayer distribution, which circumvents the ubiquitously pivotal problems of nanoparticles aggregation in the homogeneous immunoassays. Meanwhile, the enrichment effect of the substrate (about 170 NPs/μm^2) realized a denser distribution of nanoprobes than that in solution. This will amplify the detecting signal and interactive probability between the biomolecules to improve the sensitivity and detection range.

For a reliable immunoassay, UCNPs must be tightly immobilized on the substrate surface. Here, the immobilization stability of UCNPs on the substrate was characterized by the fluorescence spectra of UCNPs from 6 h to 96 h. Fig. 3b shows the I/I_O ratio of fluorescence intensity of the UCNPs-substrate after being shaken in 10 mM PBS for 0 h, 6 h, 12 h, 24 h, 48 h and 96 h. I_O and I represent the original fluorescence intensity at 542 nm and the intensity after being shaken for different periods of time, respectively. It is observed that I/I_O ratio remains almost unchanged with the time prolongation, assuring that the UCNPs bound tightly on the substrate. The stability of UCNPs fluorescence and immobilization on the substrate is in favor of accurate and reliable quantitative analysis.

GNPs were immobilized on the UCNPs-substrate through the interaction between gIgG and rIgG to construct the FRET-based detection system. The saturation of GNPs bound on the UCNPs-substrate was evaluated by monitoring the fluorescence intensity of the bio-functional substrate at different times (Fig. 3c). The energy transfer efficiency calculated by the formula $E=(I_O-I)/I_O$ is 74.4%, where I_O and I represented the fluorescence intensity of the donor in the absence and presence of the acceptor, respectively (Fig. 3d). The relatively high energy transfer efficiency is in favor of high detection

sensitivity, where FRET is the main energy transfer process, as shown in Fig. S5. Meanwhile, the stability of the bio-functional substrate is verified, as shown in Fig. S6. There are only small changes (< 4.6%) in the relative emission intensity (I/I_O) even being kept in PBS for 72 h, where I_O and I represent the original upconversion fluorescence intensity and the intensity after being kept for different times, respectively. The high stability ensures the accuracy of the immunoassay.

3.4. Quantitative analysis of gIgG in buffers

To verify the feasibility of the bio-functional substrate, we firstly attempted to analyze gIgG in buffers. When the bio-functional glass substrate was set into free gIgG solution, competitive immunoassay occurred since free gIgG would compete with gIgG-GNPs combined with rIgG-UCNPs-substrates. Consequently, some of acceptor (gIgG-GNPs) were separated away from the donor (UCNPs), resulting in the recovery of the donor fluorescence. The fluorescence spectra at different reaction times are shown in Fig. 4a, the concentration of gIgG is 60 μg/mL. And the reaction kinetics of the immunoassay is shown in Fig. 4b. After 30 min, I/I_O ratio (I for 60 μg/mL gIgG and I_O for 0 μg/mL gIgG) of fluorescence intensity reached saturation. Thus, 30 min was adopted as the optimum detection time in this assay.

For the quantitative detection of gIgG, the fluorescence spectra of the bio-functional glass substrate were measured with different free gIgG concentrations. The fluorescence spectra are shown in Fig. 4c, the fluorescence intensity gradually recovers as the concentration of gIgG increases until 60 μg/mL. The relationship between the relative fluorescence intensity $(I-I_O)/I_O$ at 542 nm and the concentration of gIgG is plotted, as shown in Fig. 4d. It shows a good linear correlation from 0.09 μg/mL to 60 μg/mL, which is a wider detection range comparing with other assays (Table S1). The coefficient of correlation (R^2) is up to 0.996. The fact proves the high reliability of this design of assay, which profits from the highly stable fluorescence of the UCNPs. The detection limit of gIgG was calculated to be 0.042 μg/mL according to the *3sb/m* criterion, where m is the slope for the range of the
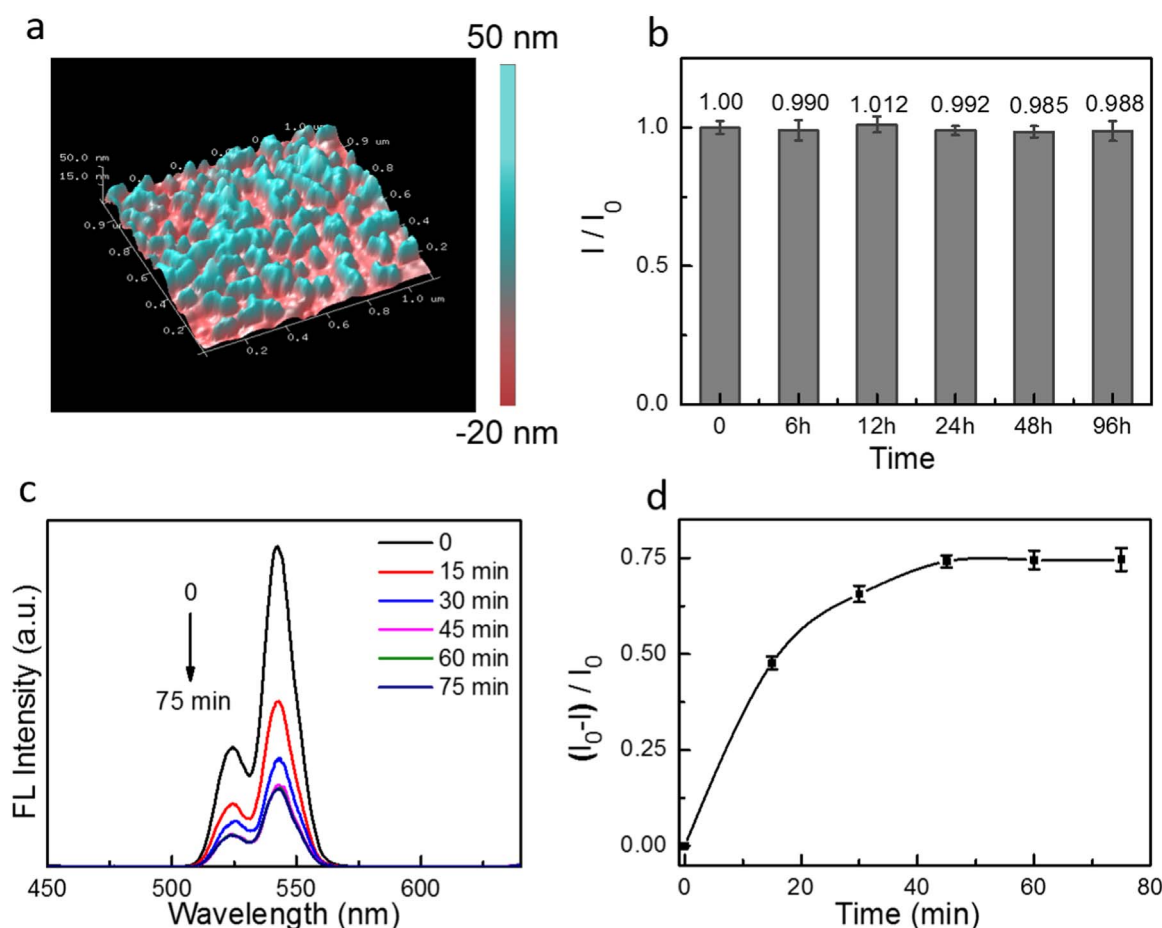
Fig. 3. (**a**) AFM image of the glass substrate surface modified with UCNPs for 24 h. (**b**) I/I_O ratio of fluorescence intensity of the UCNPs covalently immobilized on the substrate after oscillating in PBS for 0 h, 6 h, 12 h, 24 h, 48 h and 96 h, respectively. I_O and I represent the original fluorescence intensity at 542 nm and the intensity after oscillating for different period of time under excitation of 980 nm, respectively. The data is presented as average $\pm sd$ from four independent experiments. (**c**) Fluorescence spectra of the bio-functional substrate after gIgG-GNPs binding with different time, from 0 min to 75 min (**d**) $(I_O-I)/I_O$ ratio of fluorescence intensity *vs.* binding time of gIgG-GNPs with rIgG-UCNPs-substrate. I_O and I represent the fluorescence intensity of the donor (UCNPs) in the absence and presence of the acceptor (GNPs), respectively. The data is presented as average $\pm sd$ from four independent experiments.

linearity used and *sb* is the standard deviation of the blank (n=11).

Meanwhile, the absorption spectra of GNPs were analyzed. As shown in Fig. 5a, BSA-gIgG-GNPs bound with rIgG-UCNPs in solution does not cause any shift of absorption spectrum (527 nm) compared with BSA-gIgG-GNPs in solution. While the absorption spectrum of GNPs on the substrate occurs at 534 nm, which generates a red-shift of 7 nm relative to BSA-gIgG-GNPs at 527 nm, resulting from the strong interaction of the dense GNPs assembled on the substrate. The red shift of GNPs absorption spectrum is obviously beneficial to effective energy transfer, demonstrated by the overlap integral calculation (Eq. S1) with the increase of about 5%, which is in favor of a better immunoassay.

3.5. Specificity of gIgG analysis in buffers

To evaluate the specificity of the FRET-based immunoassay on the bio-functional substrate for gIgG detection, the control experiments were conducted in 10 mM PBS buffer. The influences of some other bio-molecules including rabbit-anti-human IgG, rabbit IgG, human IgG and BSA were examined. Fig. 5b shows that none of these bio-molecules causes obvious fluorescence alteration, even when the concentration is as high as 1 mg/mL for IgG and 50 mg/mL for BSA. The results clearly illustrate that the immunoassay owns excellent specificity for gIgG detection.

3.6. Quantitative analysis of gIgG in whole blood samples

To investigate the capability of the FRET-based bio-functional substrate for immunoassay directly in whole blood samples, a set of detections were conducted in 20-fold diluted whole blood solution with different amounts of gIgG. Fig. 6a displays the fluorescence spectra of the bio-functional substrate with the concentration of gIgG from 0 µg/mL to 60 µg/mL, in whole blood solution. The fluorescence intensity at 542 nm is gradually increased with increasing the concentration of gIgG, which is similar to that in buffers. Moreover, there is no obvious background signals from the whole blood samples owing to the unique fluorescence properties of UCNPs. Fig. 6b shows the relationship between the donor fluorescence recovery and gIgG concentration, a good linear relationship in 0.75 µg/mL-60 µg/mL is observed. The detection limit is calculated to be 0.51 µg/mL, slightly higher than that in buffers, and the coefficient of correlation (R^2) is 0.993, slightly lower than that in buffers. The discrepancy between buffers and whole blood may be attributed to the complexity of whole blood, decreasing the interactive probability between goat IgG and rabbit-anti-goat IgG. Additionally, the scattering and absorption from various large molecules (such as hemoglobin) and cells can also attenuate the optical signal (Hirsch et al., 2003). The results indicate that the developed bio-functional substrates are applicable for the one-step *in situ* immunoassays in low-volume whole blood samples without pre-separation of serum or plasma and multi-steps washing procedures, which shows an attractive prospect of practical applications.
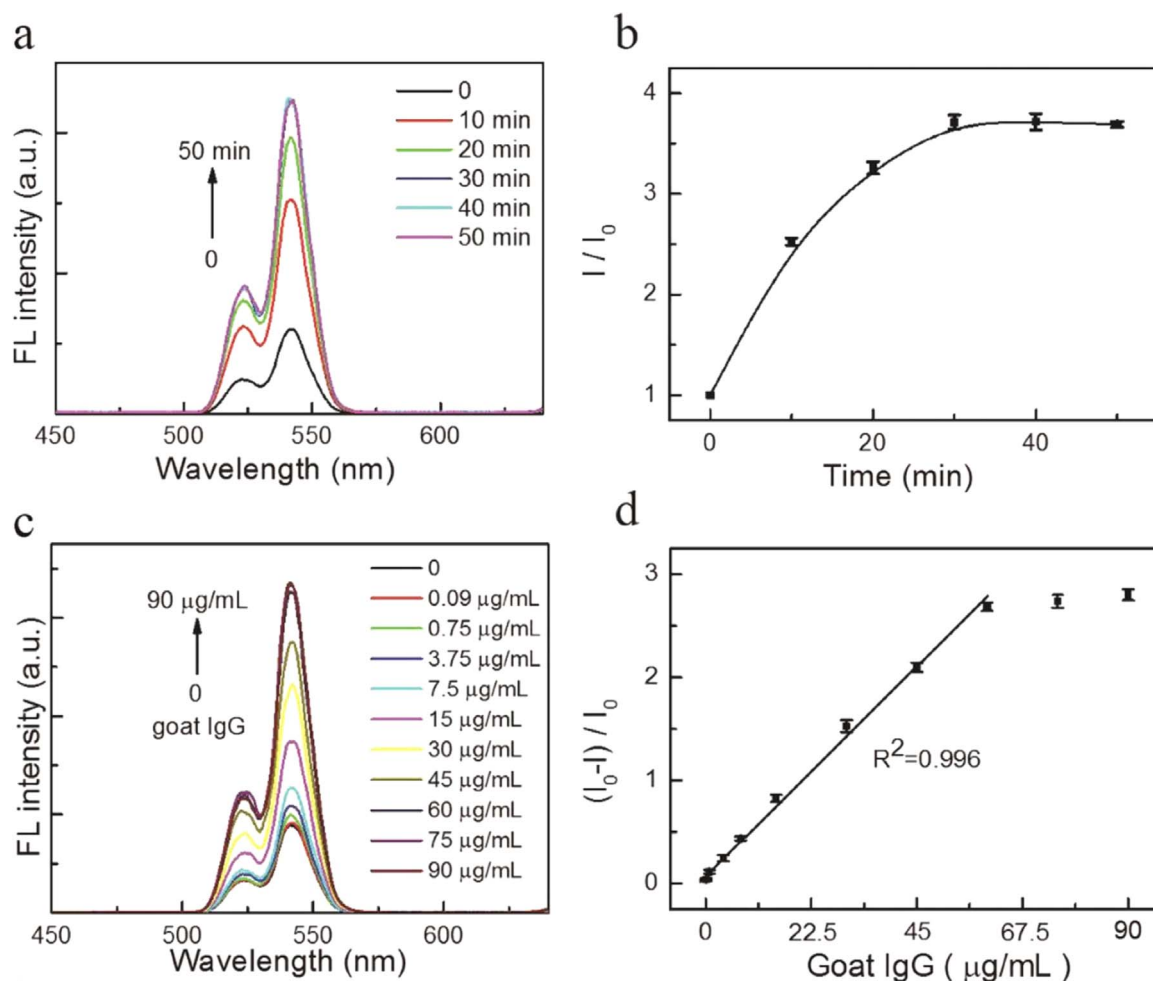
Fig. 4. (**a**) Fluorescence spectra of the FRET-based bio-functional substrate at different reaction time and (**b**) the dependence of I/I_0 ratio of fluorescence intensity on reaction time with the concentration of gIgG being 60 μg/mL. (**c**) Fluorescence spectra of the bio-functional glass substrate with increasing gIgG concentrations. (**d**) Relationship between the relative fluorescence intensity $(I-I_0)/I_0$ at 542 nm and the concentration of gIgG within the range from 0.09 μg/mL to 60 μg/mL, I_0 and I represent the fluorescence intensity of the bio-functional substrate before and after immunoassay, respectively. The data is presented as average $\pm sd$ from four independent experiments.
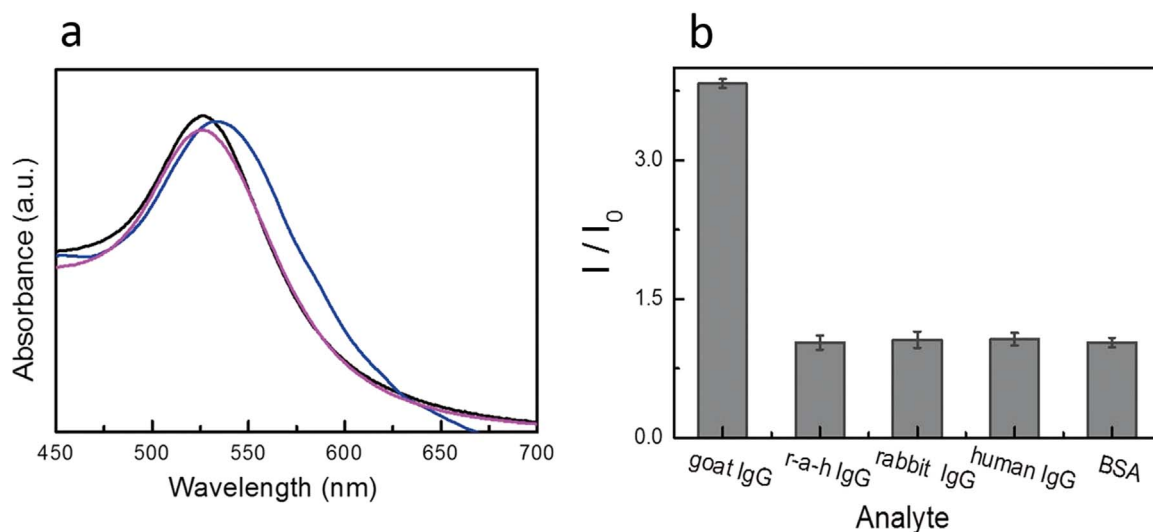

Fig. 5. (**a**) Absorption spectra of BSA-gIgG-GNPs solutions (black line), BSA-gIgG-GNPs bound with rIgG-UCNPs in solution (pink line), the BSA-gIgG-GNPs bound on UCNPs-substrate (blue line). (**b**) Relative fluorescence intensity ratio (I/I_0) of the bio-functional substrate in the presence of different analytes. The concentration of gIgG is 60 μg/mL, rabbit-anti-human IgG (r-a-h IgG), rabbit IgG, human IgG are all 1 mg/mL, and the concentration of BSA is 50 mg/mL. The data is presented as average $\pm sd$ from four independent experiments.
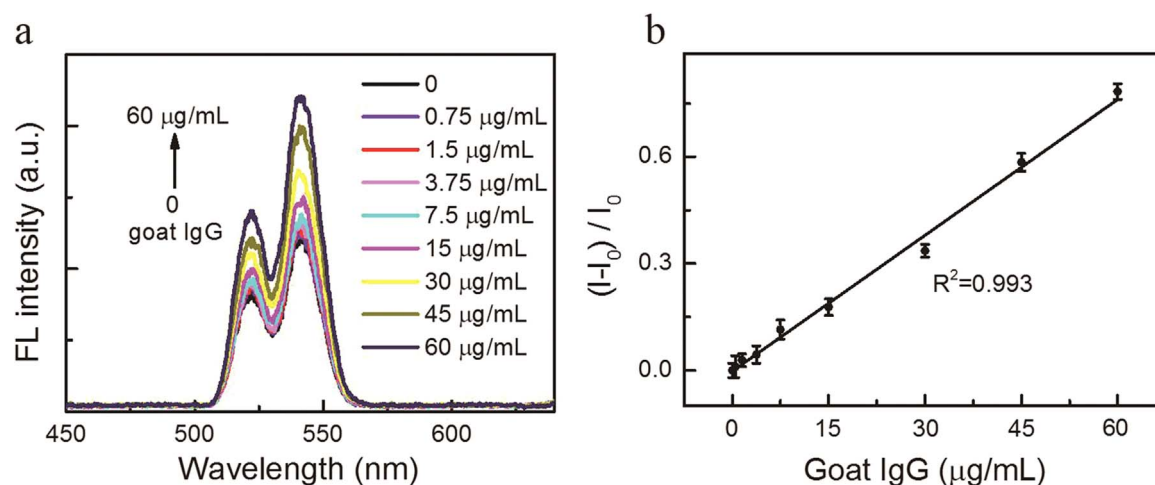
Fig. 6. (a) Fluorescence spectra of the bio-functional substrate for different concentrations of gIgG in 20-fold diluted whole blood samples. (b) Linear relationship between the relative fluorescence intensity ratio $(I-I_0)/I_0$ at 542 nm and the concentration of gIgG within the range from 0 μg/mL to 60 μg/mL, I_0 and I represent the 542 nm fluorescence intensity for different amounts of gIgG, 0 μg/mL and 0.75–60 μg/mL, respectively. The data is presented as average $\pm sd$ from four independent experiments.

4. Conclusions

In conclusion, we have successfully developed a novel one-step *in situ* immunoassay for whole blood sample detection by innovatively employing the traditional FRET in the UCNPs/rIgG/gIgG/GNPs ensemble on a substrate. It is the first one-step *in situ* immunoassay method on glass substrates, which owns a wide linear range in whole blood sample detection. This novel approach offers an attractive prospect for a rapid, sensitive and one-step *in situ* immunoassay of various bio-molecules.

Acknowledgements

Appendix A. Supplementary material

Supplementary data associated with this article can be found in the online version at doi:10.1016/j.bios.2016.11.003.

References

Algar, W.R., Krull, U.J., 2009. Anal. Chem. 81, 4113–4120.
Apilux, A., Ukita, Y., Chikae, M., Chailapakul, O., Takamura, Y., 2013. Lab Chip 13, 126–135.
Börner, S., Schwede, F., Schlipp, A., Berisha, F., Calebiro, D., Lohse, M.J., Nikolaev, V.O., 2011. Nat. Protoc. 6, 427–438.
Cen, Y., Tang, J., Kong, X., Wu, S., Yuan, J., Yu, R.Q., Chu, X., 2015. Nanoscale 7, 13951–13957.
Chen, H.Q., Yuan, F., Wang, S.Z., Xu, J., Zhang, Y.Y., Wang, L., 2013. Biosens. Bioelectron. 48, 19–25.
Clark, M.F., Adams, A.N., 1977. J. Gen. Virol. 34, 475–483.
Dulkeith, E., Ringler, M., Klar, T.A., Feldmann, J., Munoz Javier, A., Parak, W.J., 2005. Nano. Lett. 5, 585–589.
Engvall, E., Perlmann, P., 1971. Immunochemistry 8, 871–874.
Hirsch, L.R., Jackson, J.B., Lee, A., Halas, N.J., West, J.L., 2003. Anal. Chem. 75, 2377–2381.
Kim, Y., Park, S., Oh, E., Oh, Y., Kim, H., 2009. Biosens. Bioelectron. 24, 1189–1194.
Krämer, K.W., Biner, D., Frei, G., Güdel, H.U., Hehlen, M.P., Lüthi, S.R., 2004. Chem. Mater. 16, 1244–1251.
Kreisig, T., Hoffmann, R., Zuchner, T., 2011. Anal. Chem. 83, 4281–4287.
Kreyling, W.G., Abdelmonem, A.M., Ali, Z., Alves, F., Geiser, M., Haberl, N., Hartmann, R., Hirn, S., Aberasturi, D.J., Kantner, K., Khadem-Saba, G., Montenegro, J.M., Rejman, J., Rojo, T., Larramendi, I.R., Ufartes, R., Wenk, A., Parak, W.J., 2015. Nat. Nanotechnol. 10, 619–623.
Li, H., Sun, D., Liu, Y., Liu, Z., 2014. Biosens. Bioelectron. 55, 149–156.
Long, Q., Li, H., Zhang, Y., Yao, S., 2015. Biosens. Bioelectron. 68, 168–174.
Ma, H., Wu, Y., Yang, X., Liu, X., He, J., Fu, L., Wang, J., Xu, H., Shi, Y., Zhong, R., 2010. Anal. Chem. 82, 6338–6342.
Maxwell, D.J., Taylor, J.R., Nie, S., 2002. J. Am. Chem. Soc. 124, 9606–9612.
Noor, M.O., Krull, U.J., 2013. Anal. Chem. 85, 7502–7511.
Peng, J., Wang, Y., Wang, J., Zhou, X., Liu, Z., 2011. Biosens. Bioelectron. 28, 414–420.
Peng, J., Xu, W., Teoh, C.L., Han, S., Kim, B., Samanta, A., Chenger, J., Wang, L., Yuan, L., Liu, X.G., Chang, Y.T., 2015. J. Am. Chem. Soc. 137, 2336–2342.
Rantanen, T., Järvenpää, M.L., Vuojola, J., Kuningas, K., Soukka, T., 2008. Angew. Chem. Int. Ed. 120, 3871–3873.
Rivetti, C., Guthold, M., 1996. J. Mol. Biol. 264, 919–932.
Samanta, A., Zhou, Y., Zou, S., Yan, H., Liu, Y., 2014. Nano Lett. 14, 5052–5057.
Sapsford, K.E., Berti, L., Medintz, I.L., 2006. Angew. Chem. Int. Ed. 45, 4562–4589.
Tu, L., Liu, X., Wu, F., Zhang, H., 2015. Chem. Soc. Rev. 44, 1331–1345.
Wang, H., Tessmer, I., Croteau, D.L., Erie, D.A., Van-Houten, B., 2008. Nano Lett. 8, 1631–1637.
Wang, L., Yan, R., Huo, Z., Wang, L., Zeng, J., Bao, J., Wang, X., Peng, Q., Li, Y., 2005. Angew. Chem. Int. Ed. 44, 6054–6057.
Wang, Y., Jiang, K., Zhu, J., Zhang, L., Lin, H., 2015. Chem. Commun. 51, 12748–12751.
Xu, S., Xu, S., Zhu, Y., Xu, W., Zhou, P., Zhou, C., Dong, B., Song, H., 2014. Nanoscale 6, 12573–12579.
Yun, C.S., Javier, A., Jennings, T., Fisher, M., Hira, S., Peterson, S., Hopkins, B., Reich, N.O., Strouse, G.F., 2005. J. Am. Chem. Soc. 127, 3115–3119.
Zeng, Q., Zhang, Y., Song, K., Kong, X., Aalders, M.C., Zhang, H., 2009. Talanta 80, 307–312.
Zhang, F., 2015. Photon Upconversion Nanomaterials. In: Lockwood, D.J. (Ed.), Nanostructure Science and Technology. Springer, Berlin, 233–241.
Zhang, Y., Zeng, Q., Sun, Y., Liu, X., Tu, L., Kong, X., Buma, W.J., Zhang, H., 2010. Biosens. Bioelectron. 26, 149–154.